DEFLAGRATION-TO-DETONATION TRANSITION IN H2-CO-AIR MIXTURES IN A PARTIALLY OBSTRUCTED CHANNEL

Heilbronn, D.[1], Barfuss, C.[1] and Sattelmayer, T.[1]
[1] Chair of Thermodynamics, TU Munich, Boltzmannstr. 15, 85747 Garching, Germany, heilbronn@td.mw.tum.de

ABSTRACT

In this study an explosion channel is used to investigate flame dynamics in homogeneous hydrogen-carbon monoxide-air (H_2-CO-air) mixtures. The test rig is a small scale 6 m channel at a rectangular cross section of 300x60 mm. Obstacles of a blockage ratio of BR=60% and a spacing of s=300mm are placed in first part of the channel. A 2.05 m long unobstructed part in the rear of the channel allows for investigation of freely propagating flames and detonations. The fuel compostion is varied from 100/0 to 50/50 Vol.-% H_2/CO mixtures. The overall fuel content ranges from 15 to 40 Vol.-% in air aiming to obtain fast flames and deflagration-to-detonation transition (DDT). Flame speed and dynamic pressure data are evaluated. Results extend data obtained by [1] and can be used for validation of numerical frameworks. Limits for fast flames and DDT in homogeneous H_2-CO-air mixtures at the given geometry are presented.

Keywords: *fast flames, DDT, hydrogen, carbon monoxide, obstructed channel*

NOMENCLATURE

Latin

a	Speed of sound [m/s]
D	Detonation velocity [m/s]
d	Diameter [mm]
H	Channel Height [mm]
L	Length [m]
p	Pressure [Pa]
s	Spacing [mm]
t	Time [s]
u	Velocity [m/s]
W	Width [mm]
x	Distance from ignition [m]
X	Volume content [Vol.-%]

Abreviations

BR	Blockage ratio [%]
DDT	Deflagration-to-detonation transition
FA	Flame Acceleration
MCCI	Molten-Core-Concrete-Interaction
Obs.	Obstructed
Unobs.	Unobstructed

Greek

σ	Expansion ratio
ρ	Density [kg/m^3]

Subscripts

CJ	Chapman-Jouguet
D	Diffusion
F	Fuel
In	Injection
Max	Maximal
P	Products
Re	Reactants
Term	Terminal

1.0 INTRODUCTION

The share of renewable energies on the total energy supply is growing. In order to back up for power fluctuations the demand for high flexible power plants is rising. One solution to this issue might be a combination of steam reformers and gas turbines. The fuel produced by the steam reformers has high contents of Hydrogen (H_2) and Carbon Monoxide (CO), commonly known as syngas. Combustion of syngas allows for low emissions at low loads, providing high flexibility [2]. Furthermore, syngas is often found in the chemical industry as well as in gasification processes [3]. Due to its wide flammability limits and low ignition energies, flame acceleration (FA) and deflagration-to-detonation transitions (DDT) in accident scenarios pose a major danger for equipment and personnel [4].

Furthermore, the ignition of syngas-air mixtures is a key safety threat in severe accident scenarios in nuclear power plants including core meltdown and molten-core-concrete-interaction. Studies of the Fukushima-Daiichi accident showed that large amounts of H_2 and CO were produced in Unit 1 during the ex-vessel phase. Due to a failure of the containment seals, the mixture might enter the reactor building. By mixing with the ambient air, a stratified combustible mixture is formed. Ignition of the mixture destroyed the reactor building and the last barrier between the radioactive inventory and the environment [4, 5].

While former studies in the context of nuclear safety focused on FA and DDT in H_2-Air mixtures and the influence on fuel content gradients, investigations of H_2-CO-air mixtures are rare [4]. Veser investigated FA and DDT of H_2-CO-air mixtures with a partially obstructed channel of 7.2 m length, a blockage ratio of BR=30 % and a spacing of s=100 mm [1]. The investigation mainly focused on homogeneous, lean mixtures at fuel contents of $X_F \leq 15$ Vol.-%. Veser found that mixtures of 50/50 H_2/CO above $X_F > 12.5$ Vol.-% are subjected to flame acceleration reaching flames speeds above the speed of sound of the products (fast flame regime [6]). It was observed, that for fuel contents of $X_F > 13$ Vol.-% the influence of CO addition on the terminal flame speed is weak [1].

Since CFD for prediction of FA and DDT including fuel content gradients needs a wide range of validation data, investigations on a wider fuel content range is needed [7, 8]. In order to provide more knowledge about FA and DDT in H_2-CO-air mixtures the focus in this study is on fuel richer mixtures from X_F=15 Vol.-% to X_F=40 Vol.-%. Compared to Veser the channel features a different internal geometry as well as an unobstructed section.

2.0 EXPERIMENTAL SETUP

2.1 Geometry

For experimental investigation of FA and DDT in homogeneous H_2-CO-air mixtures, the GraVent test rig, as shown in figure 1, is used. The test rig is of a modular design and consists of six standard segments of 0.9 m length each and one optical segment of 0.6 m length, yielding a total length of 6 m. The channel is 60 mm in height and 300 mm in width. An optional venting volume beneath the channel was filled with wax in order to minimize its influence on the flame dynamics. The channel is partially obstructed by obstacles of a blockage ratio of BR=60 % of the cross section. Obstacles are 18 mm in height and 12 mm in width. The spacing between the obstacles is s=300 mm. The internal channel geometry was chosen in a way that flame acceleration is promoted by turbulence production by the obstacles, while DDT is not suppressed by the spacing [9]. In order to ensure sufficient flame acceleration, the length of the obstructed section is L_{obs}=3.95 m. The first obstacle is placed at a distance of x=50 mm from the end plate. The configuration of the test rig is termed BR60S300L.

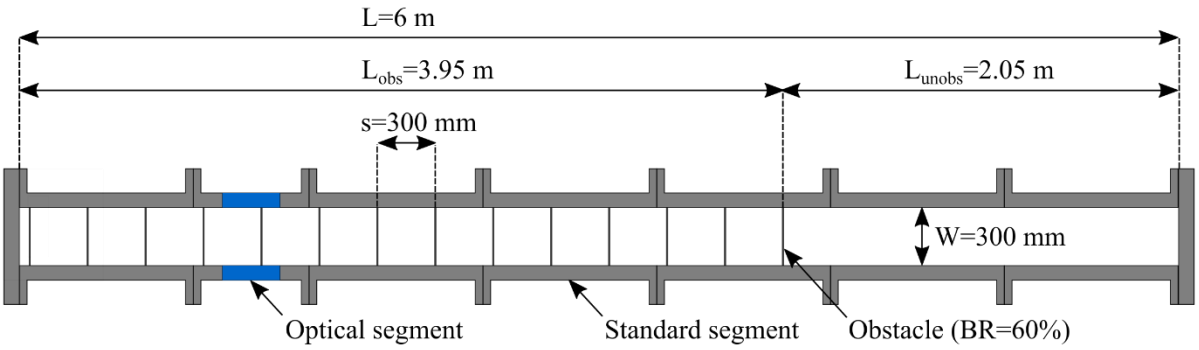

Figure 1: GraVent test rig

2.2 Experimental procedure

The fuel gas is provided to the channel by an external mixing unit, based on partial pressures. The gases are mixed in a 50 l gas cylinder, which provides the fuel to the test rig. The fuel composition was validated using a gas chromatograph, yielding a mixture accuracy of 0.5 Vol.-%. In order to ensure a steady gas flow during injection, the gas supply system features two stages of pressure reduction. The fuel is provided to the injection units at the channel at a pressure of 8 bar.

Each standard segment has three fuel distribution units providing fuel to 27 injection holes in the ceiling of the channel. The optical segment has two units. Critical flow conditions at nozzles of a diameter of d_{in}=0.9 mm upstream the fuel injection units provide a uniform fuel distribution along the channel.

Prior to injection, the channel is evacuated to a distinct vacuum. Afterwards, the fuel valves open for a fixed time in order to inject fuel into the channel to reach ambient pressure. A stratified mixture is formed due to deflection plates beneath the injection holes as shown in figure 2. In the unobstructed parts of the channel the deflection plates induce a blockage ratio of about BR=2%. Due to diffusion, the fuel distributes over the channel height, mixing with the air. The slope of the vertical fuel content is defined by the diffusion time t_D between the ending of the injection and the ignition.

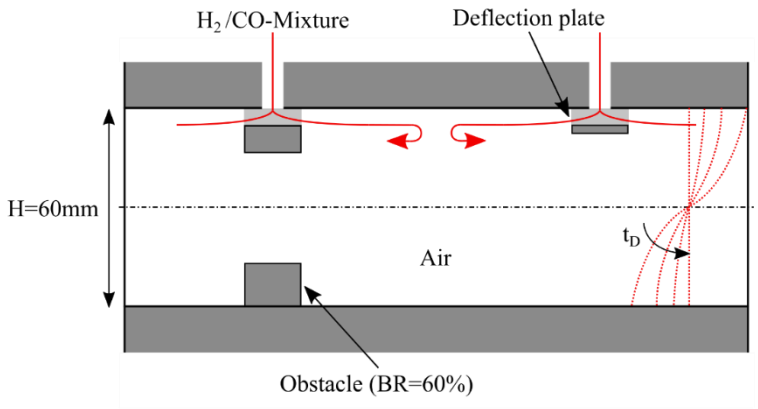

Figure 2: Injection and fuel content gradient mechanism

In order to maintain a homogeneous fuel-air mixture the diffusion time was set to t_D=60 s. Numerical studies as well as an experimental verification by gas chromatography using a model of the channel showed that the assumption of a homogeneous fuel distribution over the channel height is valid for t_D=60 s. The fuel content is determined by the pressure difference before fuel injection and before ignition. Therefore, two static pressure transducers of type SW A09 and Wika S20 are used. Due to the complex injection mechanism, small deviations in the fuel content are obtained (X_F±0.5 Vol.-%). The mixture is ignited at ambient pressure by a spark plug located at the end plate of the channel. Positions are given in terms of the axial coordinate x, starting at the ignition point.

Photodiodes and pressure transducers are used for data acquisition. 36 photodiodes are located slightly above the centerline along the channel ceiling as indicated by figure 3. The photodiodes are of type Hamamatsu S1366-18BQ. The signal of each diode is amplified by an external amplifier. The photo diodes are protected from the flame by a quartz glass cover yielding an 10° angle of view. Due to their high sensitivity in the UV, the flame is detected as it passes each diode. By combining the time and position of flame arrival, the trajectory as well as the flame velocity along the channel is obtained.

At each segment as well as at the end plate, piezo-electric pressure transducers of type Kistler 601A are installed. The pressure transducers are mounted slightly beneath the centerline. Each signal is amplified by an external Kistler 5011B amplifier. In order to protect the transducers from thermal shocks by the

flame, the face of the transducers is covered with a thin layer of high temperature silicone. Both systems are operated at a samples frequency of 250 kHz.

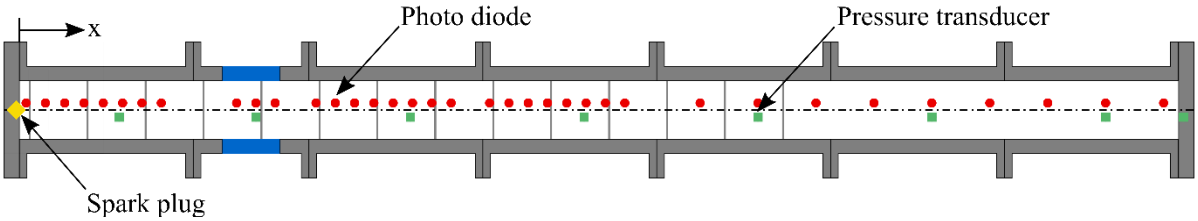

Figure 3: Sensor locations

3.0 RESULTS

The investigated fuel contents X_F as well as the corresponding expansion ratios are listed in table 1 for fuel mixtures of 100/0, 75/25 and 50/50 Vol.-% H_2/CO, respectively. The fuel content is given in Vol.-% fuel in air.

Table 1: Investigated fuel mixtures and expansion ratios

X_F [Vol.-%]	15	17.5	20	22.5	25	27.5	30	35	40
$\sigma_{100/0}$	4.64	5.14	5.62	6.06	6.47	6.81	7.02	6.88	6.58
$\sigma_{75/25}$	4.73	5.24	5.72	6.16	6.55	6.85	7.02	6.93	6.62
$\sigma_{50/50}$	4.82	5.34	5.82	6.25	6.62	6.89	7.04	7.00	6.70

The expansion ratio σ is defined as the ratio of the density of the reactants ρ_r to the density of the products, ρ_p:

$$\sigma = \frac{\rho_r}{\rho_p} \tag{1}$$

The expansion ratio can be used as a dimensionless parameter in order to assess the tendency of a mixture for flame acceleration [10, 11]. The stoichiometric composition is found at a fuel content of X_F=29.6 Vol.-%. 75/25 and 50/50 H_2/CO mixtures of X_F<15 Vol.-% could not be ignited within the test rig. Therefore results of 100/0 H_2/CO mixtures at X_F<15 Vol.-% are also not displayed.

3.1 Peak velocities and pressures

Figure 4 shows the relative maximum flame velocities $\tilde{u}_{max} = u_{max}/D_{CJ}$ measured during the investigation of the given mixtures plotted against the fuel content X_F. The flame velocity u_{max} is normalized by the Chapman-Jouguet velocity D_{CJ} for stable detonation, calculated by the Li reaction mechanism and the Shock and Detonation Toolbox [12, 13].

Most experiments show peak velocities higher than D_{CJ}. This is explained by the fact that peak velocities are found mostly within the obstacle part of the channel. Due to the interaction of the flame and the obstacles, the peak velocity partially exceeds the Chapman-Jouguet velocity, resulting in an overdriven detonation [14].

100/0 H_2-CO-air mixtures are found to have peak velocities higher than D_{CJ} for all mixtures below X_F=35 Vol.-%. The scatter becomes smaller when approaching the stoichiometric mixture at X_F=29.8 Vol.-%. For X_F=35 and X_F=40 Vol.-% the data is more scattered. For X_F≥35 Vol.-%, three out of five experiments showed peak relative velocities below D_{CJ}. The flames stay in the fast flame regime, propagating at peak velocities around the speed of sound of the products a_P [10].

For experiments of 75/25 H_2/CO mixtures below X_F=20 Vol.-%, the data is less unambiguous than for 100/0 H_2/CO mixtures. For X_F=17.5 Vol.-% both investigated mixtures are found in the fast flame regime. For X_F=15 Vol.-% and for X_F=20 Vol.-% peak relative velocities are higher than D_{CJ}. For 22.5<X_F<35 Vol.-% the majority of experiments are found to exceed D_{CJ}. In the fuel rich region above X_F=35 Vol.-%, peak velocities higher than D_{CJ} as well as fast flames are found. Relative peak velocities exceed the values of 100/0 H_2/CO.

For fuel mixtures of 50/50 H_2/CO, a similar trend is observed. For X_F<20 Vol.-% the peak relative velocities are below D_{CJ}. For fuel contents of X_F>22.5 Vol.-% almost all experiments show relative peak velocities above D_{CJ}. Especially high velocities in the fuel rich mixtures of X_F=30 Vol.-% and X_F=35 Vol.-% seem remarkable, as relative peak velocities for other mixtures are far smaller. Compared to 100/0 the majority of fuel rich mixtures for 75/25 and 50/50 H_2/CO exceed D_{CJ}.

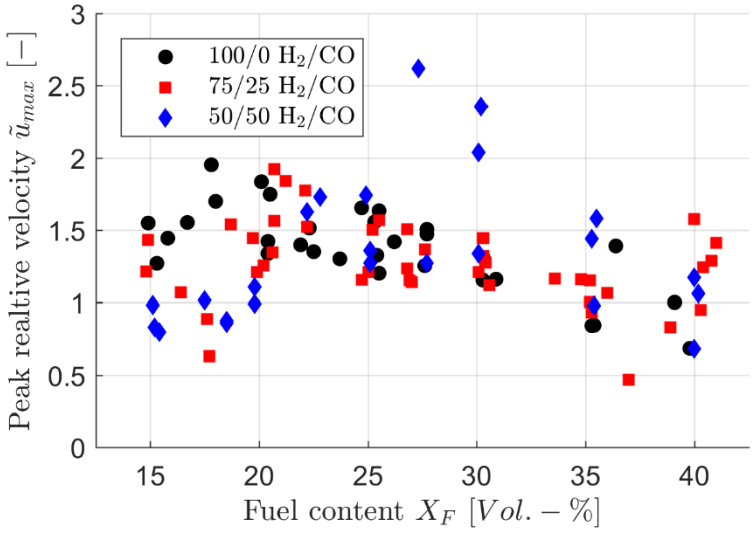

Figure 4: Peak relative flame velocity $\tilde{u}_{max} = u/D_{CJ}$ over fuel content X_f

In order to investigate flame dynamics of the mixtures at the lean and fuel rich transition limits, distance-velocity plots for X_F=20 Vol.-% as well as for X_F=35 Vol.-% are discussed in detail. The local flame velocity is obtained as described in [15].

The flame speed u plotted against the distance x for experiments at a mean fuel content of X_f=20 Vol.-% is shown in figure 5. All mixtures show similar acceleration after ignition. The 100/0 H_2/CO mixture accelerates rapidly. The flame transitions to the fast flame regime at a distance of x_{ap}=1.03 m. At a distance of x_{DCJ}=1.95 m, D_{CJ}=1709.2 m/s is exceeded. The flame speed decreases within the obstacle section showing major fluctuations. The mean velocity from x_{DCJ} to the end of the obstructed section is $\bar{u}_{obs}$=1625.9 m/s, slightly below D_{CJ}. After leaving the obstructed part, the flame accelerates to a higher mean velocity $\bar{u}_{unobs}$=1732.8 m/s. A peak velocity of u_{max}=1919.8 m/s is reached at the end of the channel.

For 75/25 H_2/CO a similar behavior is shown. After transition to the fast flame regime at x_{ap}=1.27 m, the flame speed remains slightly above the speed of sound of the products a_p=846.77 m/s. A further increase in the flame speed is recorded at a distance of x=2.55 m. After exceeding D_{CJ}=1683.6 m/s at a distance of x_{DCJ}=2.73 m, velocity fluctuations grow. The mean velocity in between x_{DCJ} and the end of the obstructed part at x=3.95 m is found to be $\bar{u}_{obs}$=1361.8 m/s, slightly below D_{CJ}. Within the unobstructed part, the flame accelerates slightly reaching a mean velocity of $\bar{u}_{Unobs}$=1583.6 m/s. The terminal velocity is slightly higher than D_{CJ} (u_{term}=1707.9 m/s).

In case of the 50/50 H_2/CO mixture, the behavior is different. The flame reaches the fast flame regime at x_{ap}=0.81 m, which is the shortest run-up distance for the compared experiments. Further increase in

velocity is observed up to x=1.7 m at u=1341.9 m/s. Afterwards major velocity fluctuations from u=246.8 m/s to u_{max}=1678 m/s at x=2.95 m are present. Within the obstructed part, the flame speed does not reach D_{CJ}=1694 m/s. After leaving the obstructed part, the flame further decelerates due to the missing turbulence induced by the obstacles to a terminal velocity of u_{term}=523.2 m/s, below the speed of sound of the products at a_p=851.26 m/s.

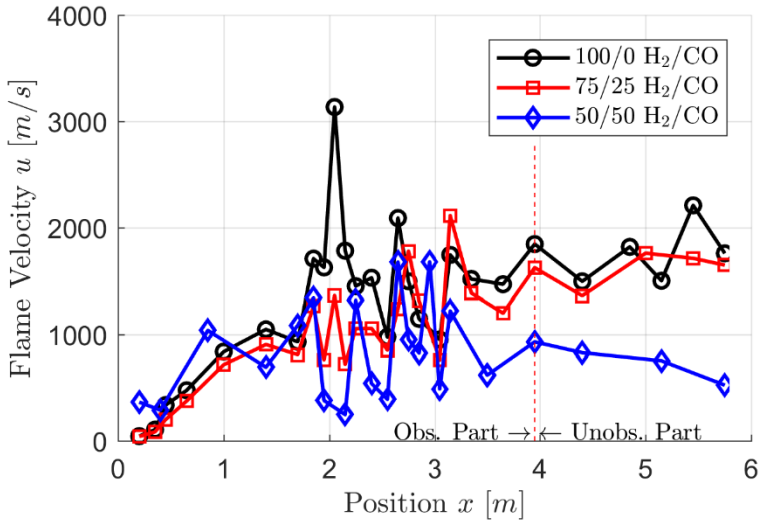

Figure 5: Flame velocity u over distance x for X_f=20.0 Vol.-%

Figure 6 shows the velocity plots for each mixture at a fuel content of X_F=35 Vol.-%. As indicated by figure 4, a different behavior is observed. For the 100/0 H_2/CO mixture the flame transitions to the fast flame regime after a run up distance of x_{ap}=1.52m. After a first local velocity maximum of u=1355 m/s, the velocity decreases, reaching a minimum of u=624.75 m/s at x=2.1 m. Starting from x=2.55 m major velocity fluctuations until the end of the obstructed section are observed, although the flame velocity does not exceed D_{CJ}. When leaving the obstructed part of the channel, the flame velocity stabilizes at a mean velocity of u=857.98 m/s, slightly below the speed of sound of the products at a_P=1007.5 m/s.

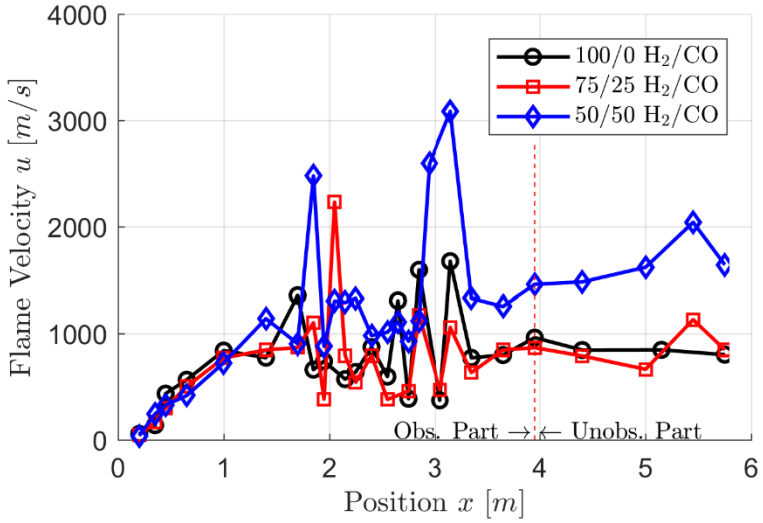

Figure 6: Flame velocity u over distance x for X_F=35.2 Vol.-%

The 75/25 H_2/CO mixture shows a slightly slower acceleration. The transition to a fast flame is observed at x_{ap}=1.77 m. A further increase to a flame speed slightly over D_{CJ} at x_{DCJ}=2.03 m is followed by a sharp decrease. A velocity fluctuation between u=471.6 m/s and u=1115 m/s is shown in the rear part of the obstructed section. The mean velocity in this part is $\bar{u}_{obs}$=728.6 m/s. In the unobstructed part a slight increase to a terminal velocity of u_{term}=846.51 m/s is measured.

For 50/50 H_2/CO the fast flame regime is reached at x_{ap}=1.25 m. D_{CJ} is exceed at a distance of x_{DCJ}=1.78 m. After a peak at x=1.85 m the flame speed decreases, showing some minor fluctuations. At x=2.95 m a second velocity peak is found, exceeding D_{CJ}. The velocity decreases in the rear part of the obstructed section. In the unobstructed part, the speed increases again, exceeding D_{CJ} at x=5.45 m.

Figure 7 shows the maximum dynamic pressure recorded during the experiments. The pressure increases as the fuel content increases from lean to stoichiometric conditions. The lowest dynamic pressures are found for a composition of 50/50 H_2/CO and a fuel content of X_F=15 Vol.-% at p_{max}=9.9 MPa. For pure hydrogen the mean dynamic pressure for X_F=15 Vol.-% is p_{max}=12.8 bar.

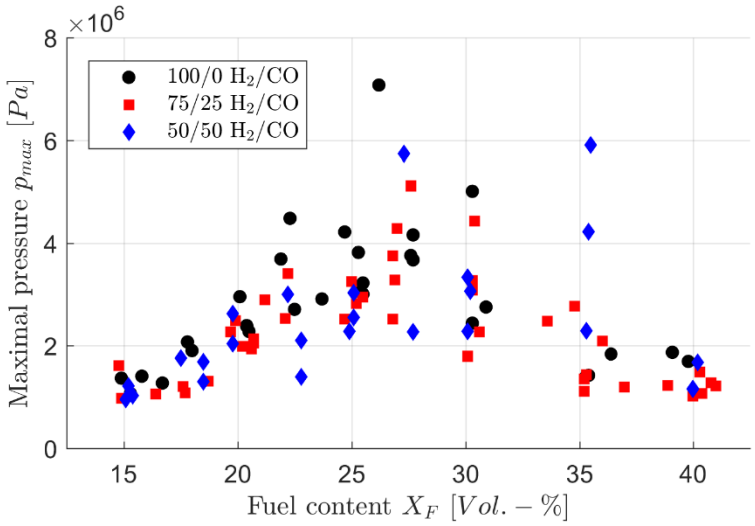

Figure 7: Maximal dynamic pressure p_{max} over fuel content X_F

As presented in figure 7, the dynamic pressure increases with increasing fuel content. A maximum is found for pure hydrogen at a fuel content of X_F=26.2 Vol.-%. For lean mixtures of X_F<20 Vol.-% fuel content, peak pressures are similar. In the region between 20 and 30 Vol.-%, the peak pressure decreases on average from $\bar{p}_{max}$=35 MPa to $\bar{p}_{max}$=30.3 MPa to $\bar{p}_{max}$=24.5 MPa for 100/0, 75/25 and 50/50 H_2/CO. The highest peak pressures at each fuel content is observed for 100/0 H_2/CO mixtures. For fuel richer mixtures, the scatter of the peak pressure increases. The highest scatter is found at contents close to the stoichiometric mixture. For fuel rich mixtures, the peak pressure decreases. A notable exception from the trend towards lower peak pressures is shown for 50/50 mixtures at X_F=35 Vol.-%. The highest peak pressure belongs to the high velocity peak at x=3 m, shown in figure 6. The mean peak pressure in the fuel rich region decreases from $\bar{p}_{max}$=28.2 MPa for 100/0 to $\bar{p}_{max}$=22.4 MPa for 75/25 H_2/CO. For 50/50 H_2/CO the mean pressure is $\bar{p}_{max}$=24.0 MPa. The rise of the mean peak pressure for 50/50 H_2/CO when compared to 75/25 H_2/CO is associated to the peaks at X_F=35 Vol.-%.

3.2 Run-up Distances

An important parameter for flame acceleration is the distance between the ignition and the location at which the flame speed reaches the speed of sound of the products. Since an acceleration to the speed of

sound of products is necessary for DDT, flames below that velocity will not transition to detonation [5, 11].

As shown in figure 8 the run-up distance to the speed of sound of the products a_P is in the range of $0.8<x_{ap}<3$ m. The mean run-up distance to fast flames in the actual configuration is calculated to $\bar{x}_{ap}$=1.13 m for 100/0, $\bar{x}_{ap}$=1.38 m for 75/25 and $\bar{x}_{ap}$=1.42 m for 50/50 H_2/CO mixtures. With exception of fuel contents of X_F=20 and X_F=35 Vol.-%, pure hydrogen mixtures show the shortest run-up distances. When compared to the run-up distance for 75/25 H_2/CO mixtures the data shows a slightly longer run-up distance. This trend becomes more evident at mixtures of 50/50 H_2/CO. Especially in a region between $22.5<X_F<30$ Vol.-% the run-up distance of 50/50 H_2/CO mixtures is in average 50% longer than for 100/0 mixtures. In the region below X_F=20 Vol.-% no clear trend is observed. While at X_F=15 Vol.-% 100/0 shows the shortest run-up distance, this trend is reversed at X_F=20 Vol.-% with the overall minimum run-up distance of x_{ap}=0.81 m for 50/50 H_2/CO. It should be noted that the mixtures of 50/50 H_2/CO showing the shortest run-up distance x_{ap} at X_F=20 Vol.-%, do not exceed D_{CJ} (see figure 5 and 9) and result in similar peak pressures (see figure 7).

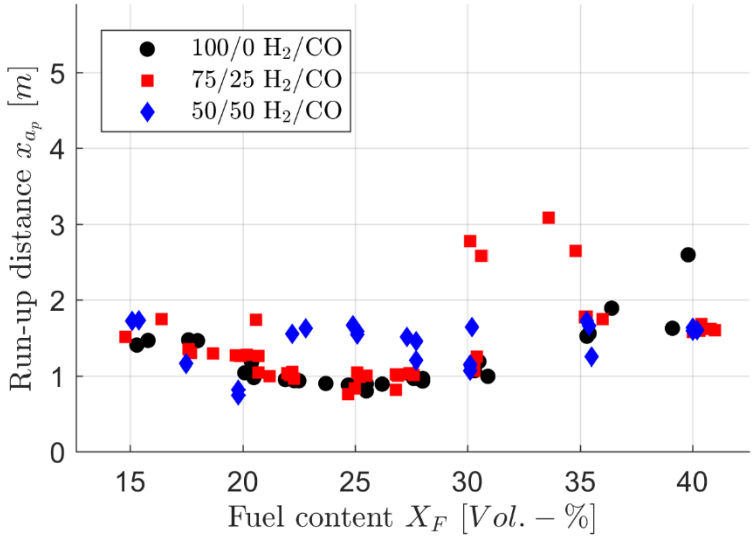

Figure 8: Run-up distance x_{ap} to speed of sound of the products a_P over fuel content X_F

For mixtures exceeding D_{CJ}, the run-up distances are plotted in figure 9. It should be noted that only two mixtures exceed D_{CJ} downstream the obstructed part. Hence, it seems that interaction with the obstacles is the main driver for DDT in the investigated mixtures. H_2-air mixtures show a sharp decrease of the run up distance at a fuel content of X_F=20 Vol.-%. As shown in figure 4, experiments at fuel contents of $X_F>30$ Vol.-% do not exceed D_{CJ} in all cases. Therefore, less run-up distance could be obtained. Scatter of the data is largest at X_F=20 and X_F=30 Vol.-%. While run-up distances at X_F=27.5 Vol.-% differ around x_{DCJ}=1.68±0.08 m, the scatter for 30 Vol.-% is found to be x_{DCJ}=2.97±1.36 m. A similar behavior is observed at X_F=20 Vol.-% at a run-up distance of x_{DCJ}=1.98±0.4 m. The mixtures seem to be more sensitive at these contents.

For experiments with 75/25 H_2/CO a similar behavior is obtained. For fuel contents $X_F<20$ Vol.-% the run-up distances are comparable to those of H_2-air mixtures. Again, a limit seems to be reached when approaching X_F=20 Vol.-%. The scatter of the run-up distance at X_F=20 Vol.-% is x_{DCJ}=2.4±1 m. For mixtures between X_F=22.5-27.5 Vol.-% the run-up distances do not differ significantly from the H_2-air mixtures and scatter is lower. For X_F=27.5 Vol.-% slightly shorter run-up distances compared to H_2-air mixtures are found (x_{DCJ}=1.4±0.15 m). For fuel contents of X_F=30 Vol.-% and X_F=35 Vol.-% the scatter increases. As displayed in figure 4, more experiments of 75/25 H_2/CO reach D_{CJ}. For X_F=40 Vol.-% the run-up distance seems to be more consistent at x_{DCJ}=2.55±0.4 m.

For 50/50 H_2/CO mixtures at X_F<20 Vol.-% most mixtures did not reach D_{CJ} (see figure 4). For X_F=22.5 Vol.-% a mean run-up distance to D_{CJ} of x_{DCJ}=2.48±0.4 m is found. For X_F=25 Vol.-% the run-up distance increases slightly to x_{DCJ}=2.86±0.14 m. For X_F=27.5 Vol.-% a slight decrease to x_{DCJ}=2.26±0.5 m is observed. Although the scatter for 50/50 H_2/CO is wider than for 75/25 and 100/0, a slight trend towards longer run-up distances is shown. For X_F=35 Vol.-% and X_F=40 Vol.-%, two out of three experiments reached D_{CJ}. The run up distance for X_F=35 Vol.-% is calculated to x_{DCJ}=1.91±0.15 m. For X_F=40 Vol.-% a slight increase is observed, reaching D_{CJ} after x_{DCJ}=2.44±0.2 m. It seems that for fuel rich mixture, 75/25 and 50/50 H_2/CO are less sensitive concerning the run-up to D_{CJ}.

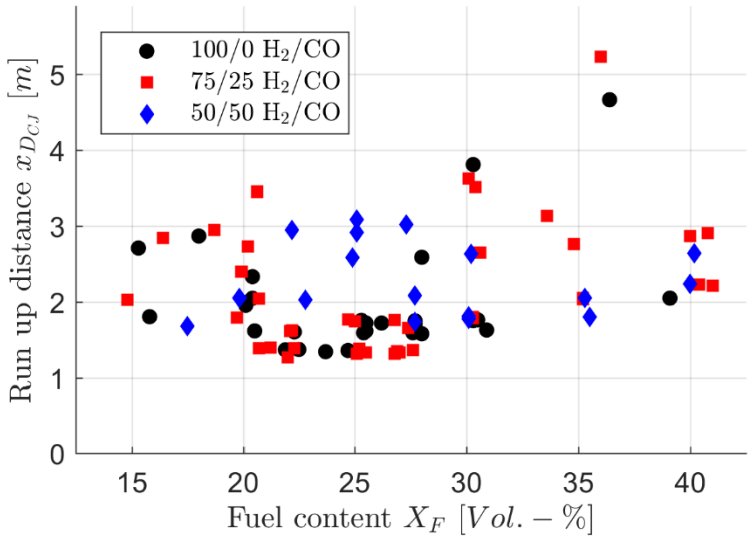

Figure 9: Run-up distance x_{DCJ} to Chapman-Jouguet velocity D_{CJ} over fuel content X_F

Figure 10 displays the mean relative terminal velocity $\tilde{u}_{term} = \bar{u}_{term}/D_{CJ}$ in the unobstructed part of the channel. The measured mean flame speed is normalized using the Chapman-Jouguet velocity D_{CJ}. Three major regimes can be distinguished: In the region X_F<20 Vol.-%, terminal velocities are found around $\tilde{u}_{term}$=0.4. In the region between 20<X_F<30 Vol.-%, terminal velocities are close to D_{CJ}. For X_F>35 Vol.-% the majority of experiments is found below $\tilde{u}_{term}$=0.5.

For 100/0 H_2/CO mixtures, the transition from the first to the second regime is found at X_F=20 Vol.-%. All mixtures of X_F>17.5 Vol.-% display terminal velocities of $\tilde{u}_{term}$=1.03, similar to 75/25 H_2/CO mixtures. For 50/50 H_2/CO the transition at X_F=20 Vol.-% is not obvious. As shown in figure 10, the transition to the second regime is shifted to higher fuel contents. For X_F=20 Vol.-%, one experiment is found closer to D_{CJ} at $\tilde{u}_{term}$=0.8. For X_F=22.5 Vol.-%, two out of three experiments are found at $\tilde{u}_{term}$=1.04.

In the second regime, the flame velocities of the investigated 100/0 H_2/CO mixtures exceed D_{CJ} in the unobstructed part of the channel between 20<X_F<30 Vol.-%. For a fuel composition of 75/25 H_2/CO the normalized terminal velocity slightly lower than $\tilde{u}_{term}$=1 is found. For a mixture of 50/50 H_2/CO the normalized terminal velocity in the second regime is found to be $\tilde{u}_{term}$=0.95. The 50/50 H_2/CO mixture shows a larger scatter of the data when compared to the 100/0 and 75/25 H_2/CO mixtures.

A turning point for all mixtures seems to be X_F=35 Vol.-%. For mixtures of X_F>35 Vol.-% a decrease in the normalized terminal velocity is observed. For 100/0 H_2/CO the normalized terminal velocity decreases from $\tilde{u}_{term}$=1 to 0.59 to 0.33 along the fuel content of X_F=30, X_F=35 and X_F=40 Vol.-%. For 75/25 H_2/CO a decrease of the normalized terminal velocity of $\tilde{u}_{term}$=0.63 to $\tilde{u}_{term}$=0.20 for X_F=35 Vol.-% and X_F=40 Vol.-% is observed. For two experiments at X_F=35 Vol.-%, relative terminal velocities in order of $\tilde{u}_{term}$=0.9 are found. For 50/50 H_2/CO this trend is shifted to X_F=40 Vol.-%. All

mixture at X_F=35 Vol.-% display a relative terminal velocity of $\tilde{u}_{term}$=0.9. A decrease to $\tilde{u}_{term}$=0.35 is found for X_F=40 Vol.-%. The scatter for the normalized terminal velocity at a fuel content of X_F=40 Vol.-% is larger than compared to 100/0 and 75/25 H_2/CO. Overall it seems, that a higher content of CO promotes higher terminal velocities in fuel rich, but lower terminal velocities in fuel lean mixtures. This could be related to higher laminar flame speeds in fuel rich H_2-CO-air mixtures. As pointed out in [2, 7] a higher CO content in H_2/CO fuels shifts the peak in laminar flame speed to higher fuel contents.

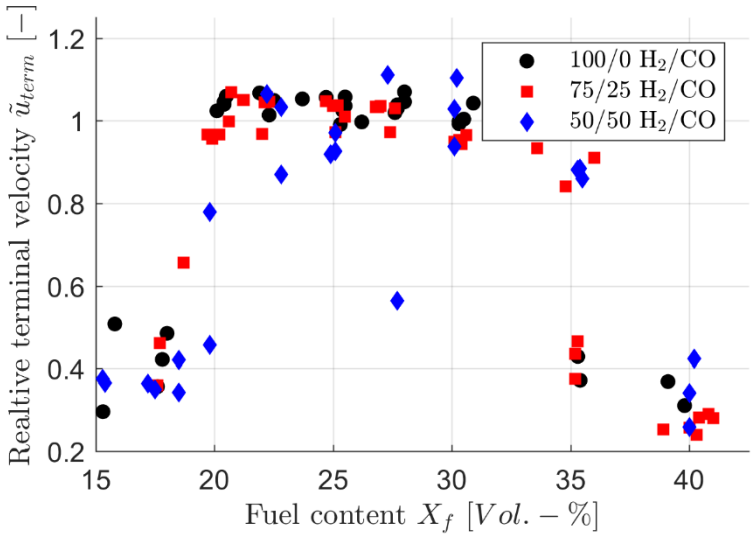

Figure 10: Relative terminal velocity $\tilde{u}_{term} = u_{term}/D_{CJ}$ over fuel content X_F

4.0 CONCLUSION AND OUTLOOK

In the present study flame acceleration and deflagration-to-detonation transition in a 100/0, 75/25 and 50/50 H_2/CO mixture were investigated. Experiments were conducted using the 6 m long GraVent test rig at BR=60 % and s=300 mm. The partially obstructed section was extended to a length of L_{obs}=3.95 m. The fuel content was varied from X_F=15-40 Vol.-%. The mixtures were investigated using pressure transducers and photo diodes in order to determine peak pressures and flame velocities.

For X_F<20 Vol.-% 75/25 and 50/50 H_2/CO show peak velocities below D_{CJ}, while 100/0 mixtures reached D_{CJ}. For fuel rich mixtures of X_F>30 Vol.-%, peak velocities for 100/0 are found below D_{CJ}, while in 75/25 and 50/50 mixtures flame speeds around D_{CJ} still occur. A similar trend is observed at the terminal velocities in the unobstructed part of the channel: 100/0 mixtures are found at terminal velocities of 0.4D_{CJ} for X_F=35 Vol.-% while for CO addition, mean terminal velocities close to D_{CJ} were observed. The observation is supported by the measured peak pressures for 75/25 and 50/50, which are found above 100/0 H_2/CO in fuel rich mixtures. The measured peak pressures show that 100/0 H_2/CO does not necessarily have to be the most dangerous mixtures concerning their hazardous potential. The study shows, that replacing CO in H_2/CO mixtures by higher H_2 contents in air [3] might result in underprediction of flame speeds and peak pressures especially in fuel rich mixtures.

Run-up distances to the fast flame regime x_{ap} are slightly longer for 75/25 and 50/50 H_2/CO mixtures. A similar trend is observed for run-up distance to D_{CJ}. The study emphasizes the importance of further investigation of flame dynamics in H_2/CO mixtures. In order to obtain generalized criteria for FA and DDT further investigations concerning the influence of the blockage ratio, the spacing and the length of the obstructed section are needed. Furthermore, studies of H_2-air mixtures revealed, that fuel content gradients have a large impact on FA and DDT [9]. Hence, it is assumed that in H_2-CO air mixtures gradients need to be considered as well. In order to gain a more detailed understanding of the phenomena, optical measurements such as Schlieren and OH-PLIF (OH-Planar laser induced fluorescence) will be used in future studies.

ACKNOWLEDGMENTS

This project is funded by the German Federal Ministry of Economics and Technology (BMWi) on the basis of a decision by the German Bundestag (project no. 1504545A) which is gratefully acknowledged.

ADDITIONAL REMARKS

An inspection of the test rig after the experiments showed, that several obstacles mounted at the ceiling of the channel in a distance of 1.5 to 3.3m from the ignition point were broken. This might result in higher uncertainties.

5.0 REFERENCES

1. Bouten, T., Beran, M. and Axelsson, L.-U., Experimental investigation of fuel composition effects on syngas combustion, *Proceedings of American Society of Mechanical Engineers Turbo Expo 2015*, 15-19 June, 2015, Montreal Canada
2. Liewen, T., Yang, V. and Yetter, R., Synthesis Gas Combustion: Fundamentals and Applications, CRC Press, Boca-Raton, 2010
3. Kumar, R.K., Koroll, G.W., Heitsch, M. and Studer, E., Carbon Monoxide-Hydrogen Combustion Characteristics in Severe Accident Containment Conditions, NEA/CSNI/R (2000)10, 2000
4. Gauntt, R., Kalinich, D., Cardoni, J., Phillips, J., Goldmann, A., Pickering, S., Francis, M., Robb, K., Ott, L., Wang, D., Smith, C., St. Germain, S. Schwieder, D. and Phelan, C., Fukushima Daiichi accident study (status of April 2012), Sandia National Laboratory Report No. SAND2012-6173.
5. Ciccarelli, G. and Dorofeev, S., Flame acceleration and transition to detonation in ducts, *Progress in energy and Combustion Science*, Vol. 34, 2008, pp. 499-550
6. Veser, A., Stern, G., Grune, J., Breitung, W. and Burgeth, B., Co-H2-Air-Combustion Tests in the FKZ -7 m –Tube, Programm Nukleare Sicherheitsforschung, Jahresbericht 2001, Teil 1, Bericht FZKA-6741, 2002
7. Barfuss, C., Heilbronn, D. and Sattelmayer, T., Numerical Simulation of Deflagration and Detonation of Homogeneous Hydrogen-Carbon Monoxide-Air Mixtures, *Proceedings of the 12th International Symposium on Hazards, Prevention and Mitigation of Industrial Explosions (ISHPMIE)*, 12-17 August, 2018, Kansas City, USA, in print
8. Barfuss, C., Heilbronn, D. and Sattelmayer, T., Simulation of Deflagration-to-Detonation Transition of Lean H2-CO-Air Mixtures in Obstructed Channels, *Proceedings of the International Conference on Hydrogen Safety*, 24-26 September, 2019, Adelaide, Australia, in print
9. Vollmer, K.G., Ettner, F. and Sattelmayer, T., Influence of Concentration Gradients on Flame Acceleration in Tubes, *Proceedings of the 8th International Symposium on Hazards, Prevention and Mitigation of Industrial Explosions (ISHPMIE)*, 5-10 September, 2010, Yokohama, Japan
10. Lee, J.H.S., The Detonation Phenomenon, 2008, Cambridge University Press, New York
11. Breitung, W., Chan, C., Dorofeev, S., Eder, A., Gelfand, B., Heitsch, M., Klein, R., Mallaikos, A., Shepherd, E., Studer, E. and Thibault, P., State-of-the-Art Report On Flame Acceleration And Deflagration-to-Detonation Transition In Nuclear Safety, NEA/CSNI/R(2000)7, 2000
12. Li, X., You, X., Wi, F., Law, C. K., Uncertainty analysis of the kinetic model prediction for high pressure H2/CO combustion, *Proceedings of the Combustion Institute*, Vol. 35, Issue 1, 2015, pp. 617-624
13. California Institute of Technology, Shock and Detonation Toolbox, http://shepherd.caltech.edu/EDL/PublicResources/sdt/
14. Eder, A., Brennverhalten schallnaher und überschallschneller Wasserstoff-Luft-Flammen, PhD Thesis, Technical University Munich, 2001
15. Vollmer, K., Einfluss von Mischungsgradienten auf die Flammenbeschleunigung und die Detonation in Kanälen, PhD Thesis, Technical University Munich, 2015